On the Identities for Elastostatic Fundamental Solution and Nonuniqueness of the Traction BIE Solution for Multiconnected Domains

Y. J. Liu[1]
Mechanical Engineering,
University of Cincinnati,
Cincinnati, OH 45221-0072
e-mail: Yijun.Liu@uc.edu

W. Ye

Y. Deng

Mechanical Engineering,
Hong Kong University of Science and Technology,
Hong Kong

In this paper, the four integral identities satisfied by the fundamental solution for elastostatic problems are reviewed and slightly different forms of the third and fourth identities are presented. Two new identities, namely the fifth and sixth identities, are derived. These integral identities can be used to develop weakly singular and nonsingular forms of the boundary integral equations (BIEs) for elastostatic problems. They can also be employed to show the nonuniqueness of the solution of the traction (hypersingular) BIE for an elastic body on a multiconnected domain. This nonuniqueness is shown in a general setting in this paper. It is shown that the displacement (singular) BIE does not allow any rigid-body displacement terms, while the traction BIE can have arbitrary rigid-body translation and rotation terms, in the BIE solutions on the edge of a hole or surface of a void. Therefore, the displacement solution from the traction BIE is not unique. A remedy to this nonuniqueness solution problem with the traction BIE is proposed by adopting a dual BIE formulation for problems with multiconnected domains. A few numerical examples using the 2D elastostatic boundary element method for domains with holes are presented to demonstrate the uniqueness properties of the displacement, traction and the dual BIE solutions for multiconnected domain problems. [DOI: 10.1115/1.4023640]

Keywords: integral identities, fundamental solution, elastostatics, boundary integral equation, boundary element method

1 Introduction

The boundary element method (BEM) has been applied for solving elastostatic problems for almost five decades based on the direct boundary integral equation (BIE) formulation [1]. Although very attractive and successful in solving many elastostatic problems, especially with the recent advent of the fast solution methods [2], the BIE formulations for elastostatics suffer some defects for certain problems. For example, for plane elasticity problems, the displacement BIE has nonunique solutions for certain types of domain [3]; the displacement BIE degenerates when applied to domains containing cracks (see, e.g., Refs. [4,5]); and the traction BIE has nonunique solutions on the edges of holes or surfaces of voids in a multiconnected domain, which is the topic of this paper.

For multiconnected domain elasticity and Stokes flow problems, it has been demonstrated that the traction or hypersingular BIEs have nonunique solutions on the boundary of a hole or void where no constraint is applied. That is, an arbitrary translation and/or rotation term can be added to the solution of the displacement on the boundary of the hole or void and the traction BIE solution still holds. This is because of the properties of the hypersingular kernels, or the identities satisfied by such kernels [6–8]. This defect in the traction BIEs for multiconnected domains was reported in Refs. [9,10] for elasticity problems, and in Refs. [11,12] for Stokes flow problems. Special care or techniques were also proposed in Refs. [9,10] to remedy this situation with the traction BIE for multiconnected domain elasticity problems. For Stokes flow problems, a dual BIE formulation using a linear combination of the singular and hypersingular BIEs is suggested in Refs. [11,12].

However, the above mentioned nonuniqueness problem of the traction BIE solution has not been investigated in a general setting, meaning that no paper has shown the nonuniqueness of the traction BIE solution that can have both arbitrary constant and linear terms and for both 2D and 3D multiconnected domains. In this paper, the issue of the nonunique solution with the direct BIE formulation for elastostatic problems on multiconnected domains is investigated using a general approach. To do this, two new integral identities for the fundamental solution of elastostatic problems are derived. Then, it is shown that the displacement BIE solution does not admit constant and linear terms, while the traction BIE solution can have such terms and therefore is not unique on the edge of a hole or surface of a void. These results are consistent with those for the BIEs for multiconnected domain elasticity problems. However, these results are derived in a systematic manner and under general conditions.

The remaining part of this paper is organized as following. In Sec. 2, the four integral identities are reviewed and new forms of the third and fourth identities are presented. Two new identities are derived which are named as the fifth and sixth identities. In Sec. 3, the nonuniqueness issue of the solutions of the BIEs for multiconnected domain problems is investigated using the derived integral identities. A remedy to the nonuniqueness problem is proposed using a dual BIE formulation. In Sec. 4, the matrix notation is applied to further demonstrate the nonuniqueness of the traction BIE solutions for domains with holes or voids. In Sec. 5, a few numerical examples of 2D elastic bodies with holes solved using the

[1]Corresponding author.
Manuscript received September 12, 2012; final manuscript received December 27, 2012; accepted manuscript posted February 12, 2013; published online July 12, 2013. Assoc. Editor: Glaucio H. Paulino.

BEM are presented to demonstrate the correctness of the dual BIE approach for multiconnected domains. Section 6 concludes the paper.

2 Identities for the Fundamental Solution

The stress component $\Sigma_{ijk}(\mathbf{x},\mathbf{y})$ at a field point $\mathbf{y}$ in the elastostatic fundamental solution (Kelvin's solution) satisfies the following governing equation:

$$\Sigma_{ijk},_k(\mathbf{x},\mathbf{y}) + \delta_{ij}\delta(\mathbf{x},\mathbf{y}) = 0, \quad \forall \mathbf{x},\mathbf{y} \in R^2 \text{ or } R^3 \tag{1}$$

where $(),_k = \partial()/\partial y_k$, the first index i indicates the direction of a unit concentrated force at the source point $\mathbf{x}$, the Dirac-δ function $\delta(\mathbf{x},\mathbf{y})$ represents the body force corresponding to this unit concentrated force, and R^2 or R^3 represents the 2D or 3D full space, respectively.

The displacement component $U_{ij}(\mathbf{x},\mathbf{y})$ and traction component $T_{ij}(\mathbf{x},\mathbf{y})$ (also called kernels) in the fundamental solution satisfy the following integral identities (see Refs. [6–8] for derivations):

First identity:

$$\int_\Gamma T_{ij}(\mathbf{x},\mathbf{y})d\Gamma(\mathbf{y}) = \begin{cases} -\delta_{ij}, & \forall \mathbf{x} \in \Omega \\ -\frac{1}{2}\delta_{ij}, & \forall \mathbf{x} \in \Gamma \\ 0, & \forall \mathbf{x} \in \mathrm{E} \end{cases} \tag{2}$$

Second identity:

$$\int_\Gamma \frac{\partial T_{ij}(\mathbf{x},\mathbf{y})}{\partial x_k} d\Gamma(\mathbf{y}) = 0, \quad \forall \mathbf{x} \in R^2 \text{ or } R^3 \tag{3}$$

Third identity:

$$E_{jkpq}\int_\Gamma \frac{\partial U_{ip}(\mathbf{x},\mathbf{y})}{\partial x_l} n_q(\mathbf{y})d\Gamma(\mathbf{y}) - \int_\Gamma \frac{\partial T_{ij}(\mathbf{x},\mathbf{y})}{\partial x_l}(y_k - \bar{y}_k)d\Gamma(\mathbf{y}) = \begin{cases} \delta_{ij}\delta_{kl}, & \forall \mathbf{x} \in \Omega \\ \frac{1}{2}\delta_{ij}\delta_{kl}, & \forall \mathbf{x} \in \Gamma \\ 0, & \forall \mathbf{x} \in \mathrm{E} \end{cases} \tag{4}$$

Fourth identity:

$$E_{jkpq}\int_\Gamma U_{ip}(\mathbf{x},\mathbf{y})n_q(\mathbf{y})d\Gamma(\mathbf{y}) - \int_\Gamma T_{ij}(\mathbf{x},\mathbf{y})(y_k - \bar{y}_k)d\Gamma(\mathbf{y}) = \begin{cases} \delta_{ij}(x_k - \bar{y}_k), & \forall \mathbf{x} \in \Omega \\ \frac{1}{2}\delta_{ij}(x_k - \bar{y}_k), & \forall \mathbf{x} \in \Gamma \\ 0, & \forall \mathbf{x} \in \mathrm{E} \end{cases} \tag{5}$$

where Γ is a smooth closed contour (for 2D) or surface (for 3D), Ω is the domain enclosed by Γ, E is the infinite domain outside Γ ($\Omega \cup \Gamma \cup \mathrm{E} = R^2$ or R^3), E_{ijkl} is the Young's modulus tensor, and $\bar{y}_k$ is the coordinate of a fixed reference point $\mathbf{y}$ in space. Note that in the third and fourth identities derived in Refs. [6–8], $\bar{y}_k = x_k$, which are special cases of identities [4] and [5]. The new forms of the third and fourth identities in Refs. [4] and [5] will be convenient when we prove the nonuniqueness of the traction BIE for multiconnected domain problems.

All the above identities can be derived readily by integrating governing Eq. (1) over the domain Ω in the following manner [6–8]:

$$\int_\Omega (y_m - \bar{y}_m)^\alpha \frac{\partial^\gamma}{\partial x_l^\gamma}\left[\Sigma_{ijk},_k(\mathbf{x},\mathbf{y}) + \delta_{ij}\delta(\mathbf{x},\mathbf{y})\right]d\Omega(\mathbf{y}) = 0, \quad \forall \mathbf{x},\mathbf{y} \in R^2 \text{ or } R^3 \tag{6}$$

for selected integers α and γ and invoking the Gauss theorem. Knowledge of the explicit expressions of the displacement and traction kernels and the associated BIEs is not required in the development of these identities, although they can also be derived by imposing simple solutions to the BIEs [6–8,13–15]. It is also noted that the second identity, Eq. (3), can be derived by taking the derivative of the first identity, Eq. (2), and the third identity, Eq. (4), can be obtained by taking the derivative of the fourth identity, Eq. (5). These identities have physical meanings and can be very convenient in deriving various weakly singular or nonsingular forms of the BIEs for elasticity problems [6–8].

Two new identities can be derived readily from the above existing identities. Since the Young's modulus tensor satisfies $E_{ijkl} = E_{jikl} = E_{ijlk} = E_{klij}$, we can switch the indices j and k in the fourth identity, Eq. (5), and subtract the result from the original one to obtain the following:

Fifth identity:

$$\int_\Gamma T_{ik}(\mathbf{x},\mathbf{y})(y_j - \bar{y}_j)d\Gamma(\mathbf{y}) - \int_\Gamma T_{ij}(\mathbf{x},\mathbf{y})(y_k - \bar{y}_k)d\Gamma(\mathbf{y}) = \begin{cases} \delta_{ij}(x_k - \bar{y}_k) - \delta_{ik}(x_j - \bar{y}_j), & \forall \mathbf{x} \in \Omega \\ \frac{1}{2}\left[\delta_{ij}(x_k - \bar{y}_k) - \delta_{ik}(x_j - \bar{y}_j)\right], & \forall \mathbf{x} \in \Gamma \\ 0, & \forall \mathbf{x} \in \mathrm{E} \end{cases} \tag{7}$$

A special version of this identity was derived in Ref. [10] for the 2D case based on a physical argument (equilibrium of moments of the traction) and with $\bar{y}_j = 0$.

Taking the derivative of the new identity, Eq. (7), with respective to x_l, we obtain the following:

Sixth identity:

$$\int_\Gamma \frac{\partial T_{ik}(\mathbf{x},\mathbf{y})}{\partial x_l}(y_j - \bar{y}_j)d\Gamma(\mathbf{y}) - \int_\Gamma \frac{\partial T_{ij}(\mathbf{x},\mathbf{y})}{\partial x_l}(y_k - \bar{y}_k)d\Gamma(\mathbf{y}) = \begin{cases} \delta_{ij}\delta_{kl} - \delta_{ik}\delta_{jl}, & \forall \mathbf{x} \in \Omega \\ \frac{1}{2}\left[\delta_{ij}\delta_{kl} - \delta_{ik}\delta_{jl}\right], & \forall \mathbf{x} \in \Gamma \\ 0, & \forall \mathbf{x} \in \mathrm{E} \end{cases} \tag{8}$$

This new identity can also be derived from the third identity, Eq. (4), by switching the indices j and k and subtracting the result from the original one. The two new identities, Eqs. 7 and (8), will be applied in the following section to prove the nonuniqueness of the traction BIE for multiconnected domain problems.

3 Nonuniqueness of the Solution With the Traction BIE for Multiconnected Domains

Consider an elastostatic problem on a multiconnected domain V (Fig. 1). The displacement (singular) BIE is [1]

$$\frac{1}{2}u_i(\mathbf{x}) = \int_S \left[U_{ij}(\mathbf{x},\mathbf{y})t_j(\mathbf{y}) - T_{ij}(\mathbf{x},\mathbf{y})u_j(\mathbf{y})\right]dS(\mathbf{y}), \quad \forall \mathbf{x} \in S \tag{9}$$

where u_i and t_i are the displacement and traction on boundary S, respectively. The body force is not considered and the boundary S is assumed to be smooth in this paper, which will not alter the conclusions. The traction (hypersingular) BIE is [12,16]

$$\frac{1}{2}t_i(\mathbf{x}) = \int_S \left[K_{ij}(\mathbf{x},\mathbf{y})t_j(\mathbf{y}) - H_{ij}(\mathbf{x},\mathbf{y})u_j(\mathbf{y})\right]dS(\mathbf{y}), \quad \forall \mathbf{x} \in S \tag{10}$$

where the two new kernels are given by

$$K_{ij}(\mathbf{x},\mathbf{y}) = E_{ikpq}\frac{\partial U_{pj}(\mathbf{x},\mathbf{y})}{\partial x_q}n_k(\mathbf{x}), \quad H_{ij}(\mathbf{x},\mathbf{y}) = E_{ikpq}\frac{\partial T_{pj}(\mathbf{x},\mathbf{y})}{\partial x_q}n_k(\mathbf{x}) \tag{11}$$

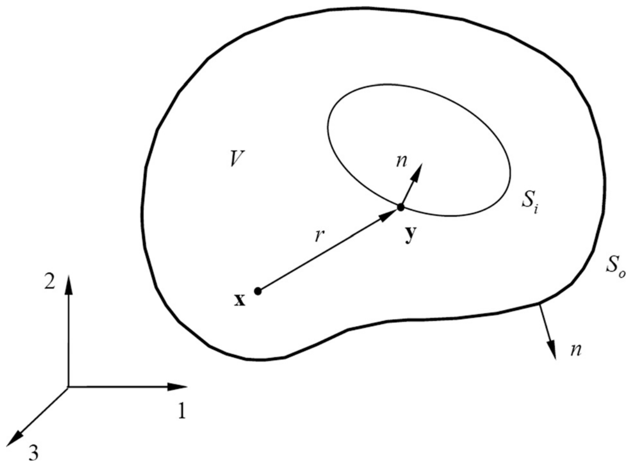

Fig. 1 A multiconnected domain *V* with outer boundary S_o and inner boundary $S_i S_o \cup S_i = S$)

We now investigate the solutions of displacement BIE Eq. (9) and traction BIE Eq. (10) for multiconnected domains (Fig. 1) to see if the solutions are unique or not on the inner boundary (the edge of a hole in 2D or surface of a void in 3D). In Fig. 1, S_o is the outer boundary and S_i is a typical inner boundary which is not constrained.

Assume $u_i(\mathbf{y})$ is a solution to BIE Eq. (9), or BIE Eq. (10). We consider the following field:

$$\widetilde{u}_i(\mathbf{y}) = \begin{cases} u_i(\mathbf{y}), & \mathbf{y}\in S_o \\ u_i(\mathbf{y}) + \left[c_i + d_{ij}(y_j - \bar{y}_j)\right], & \mathbf{y}\in S_i \end{cases} \tag{12}$$

which is obtained by adding a constant solution c_i and linear solution $d_{ij}(y_j - \bar{y}_j)$ to $u_i(\mathbf{y})$ on the inner boundary S_i. The constant solution c_i represents a rigid-body translation, while the linear term $d_{ij}(y_j - \bar{y}_j)$ can produce a constant strain field given by

$$\bar{\varepsilon}_{ij} = \frac{1}{2}(d_{ij} + d_{ji}) \tag{13}$$

The linear term $d_{ij}(y_j - \bar{y}_j)$ can represent a rigid-body rotation only if the following condition is satisfied:

$$d_{ij} = -d_{ji} \tag{14}$$

which ensures zero strain and stress arising from this linear term. In the following, we assume that condition, Eq. (14), is satisfied.

We first investigate if the field in Eq. (12) (satisfying condition, Eq. (14)) is also a solution of the displacement BIE, Eq. (9). To do this, substituting $\widetilde{u}_i(\mathbf{y})$ into displacement BIE, Eq. (9), with $\mathbf{x}\in S_o$ first, we have

$$\frac{1}{2}u_i(\mathbf{x}) = \int_{S_o\cup S_i}\left[U_{ij}(\mathbf{x},\mathbf{y})t_j(\mathbf{y}) - T_{ij}(\mathbf{x},\mathbf{y})u_j(\mathbf{y})\right]dS(\mathbf{y})$$
$$\int_{S_i}\left\{-T_{ij}(\mathbf{x},\mathbf{y})\left[c_j + d_{jk}(y_k - \bar{y}_k)\right]\right\}dS(\mathbf{y}), \quad \forall\mathbf{x}\in S_o$$

which is reduced to

$$0 = -c_j\int_{S_i}T_{ij}(\mathbf{x},\mathbf{y})dS(\mathbf{y}) - d_{jk}\int_{S_i}T_{ij}(\mathbf{x},\mathbf{y})(y_k - \bar{y}_k)dS(\mathbf{y}), \quad \mathbf{x}\in S_o \tag{15}$$

by applying BIE Eq. (9) for $u_i(\mathbf{y})$. The above equation is further reduced to

$$-d_{jk}\int_{S_i}T_{ij}(\mathbf{x},\mathbf{y})(y_k - \bar{y}_k)dS(\mathbf{y}) = 0, \quad \mathbf{x}\in S_o$$

for any values of c_j, by using the first identity, Eq. (2), applied to the domain enclosed by S_i with $\mathbf{x}$ outside this domain and after switching the direction of the normal on S_i (Fig. 2). Note that when the direction of the normal is reversed on S_i (Fig. 2(*b*)), which is required before we can apply the identities, $T_{ij}(\mathbf{x},\mathbf{y})$ changes sign. We do not use a different symbol for normal n after the direction is switched, in order to simplify the notation. Splitting the kernel in the integral in the above equation into two and applying the condition in Eq. (14), we have

$$\frac{1}{2}d_{jk}\int_{S_i}\left[T_{ik}(\mathbf{x},\mathbf{y})(y_j - \bar{y}_j) - T_{ij}(\mathbf{x},\mathbf{y})(y_k - \bar{y}_k)\right]dS(\mathbf{y}) = 0, \quad \mathbf{x}\in S_o \tag{16}$$

which is satisfied by the new fifth identity, Eq. (7), for any values of d_{jk}.

Similarly, substituting $\widetilde{u}_i(\mathbf{y})$ into displacement BIE Eq. (9) with $\mathbf{x}\in S_i$, we obtain

$$\frac{1}{2}\delta_{ij}\left[c_j + d_{jk}(x_k - \bar{y}_k)\right] = \int_{S_i}\left\{-T_{ij}(\mathbf{x},\mathbf{y})\left[c_j + d_{jk}(y_k - \bar{y}_k)\right]\right\}dS(\mathbf{y}),$$
$$\mathbf{x}\in S_i \tag{17}$$

by applying BIE Eq. (9) for $u_i(\mathbf{y})$. After reversing the direction of the normal (Fig. 2(*b*)), this equation is changed to

$$c_j\left[\frac{1}{2}\delta_{ij} - \int_{S_i}T_{ij}(\mathbf{x},\mathbf{y})dS(\mathbf{y})\right] + d_{jk}\left[\frac{1}{2}\delta_{ij}(x_k - \bar{y}_k)\right.$$
$$\left. - \int_{S_i}T_{ij}(\mathbf{x},\mathbf{y})(y_k - \bar{y}_k)dS(\mathbf{y})\right] = 0, \quad \mathbf{x}\in S_i$$

or

$$c_j\left[\frac{1}{2}\delta_{ij} - \int_{S_i}T_{ij}(\mathbf{x},\mathbf{y})dS(\mathbf{y})\right] + d_{jk}\left\{\frac{1}{2}\delta_{ij}(x_k - \bar{y}_k)\right.$$
$$\left. + \frac{1}{2}\int_{S_i}\left[T_{ik}(\mathbf{x},\mathbf{y})(y_j - \bar{y}_j) - T_{ij}(\mathbf{x},\mathbf{y})(y_k - \bar{y}_k)\right]dS(\mathbf{y})\right\} = 0, \ \mathbf{x}\in S_i$$

by splitting the kernel in the second integral and applying the condition in Eq. (14). Using the first identity, Eq. (2) and fifth identity, Eq. (7), we have from the above equation

$$c_j\left[\frac{1}{2}\delta_{ij} + \frac{1}{2}\delta_{ij}\right] + d_{jk}\left\{\frac{1}{2}\delta_{ij}(x_k - \bar{y}_k) + \frac{1}{4}\left[\delta_{ij}(x_k - \bar{y}_k) - \delta_{ik}(x_j - \bar{y}_j)\right]\right\} = 0,$$
$$\mathbf{x}\in S_i$$

or

$$c_i + d_{ik}(x_k - \bar{y}_k) = 0, \ \mathbf{x}\in S_i \tag{18}$$

by applying again the condition in Eq. (14). The above equation cannot be satisfied with arbitrary values of c_i, d_{ik} and x_k, unless

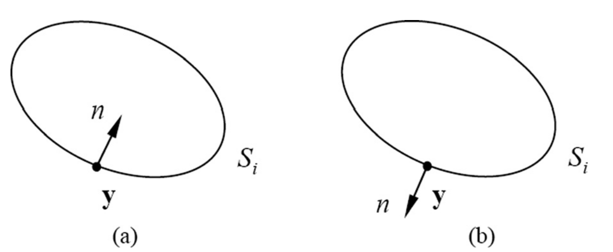

Fig. 2 Reversing the direction of the normal on S_i before applying the identities

$c_i = 0$ and $d_{ik} = 0$. This shows that the displacement BIE solution cannot admit any rigid-body translation or rotation terms on the edge of a hole or surface of a void. Therefore, the displacement BIE solution on the edge of a hole or the surface of a void is unique for multiconnected domain problems.

Next, substituting $\tilde{u}_i(\mathbf{y})$ into traction BIE Eq. (10) with $\mathbf{x} \in S_o$, we have

$$\frac{1}{2}t_i(\mathbf{x}) = \int_{S_o \cup S_i} \left[K_{ij}(\mathbf{x},\mathbf{y})t_j(\mathbf{y}) - H_{ij}(\mathbf{x},\mathbf{y})u_j(\mathbf{y})\right]dS(\mathbf{y}) \int_{S_i} \left\{-H_{ij}(\mathbf{x},\mathbf{y})\left[c_j + d_{jk}(y_k - \bar{y}_k)\right]\right\}dS(\mathbf{y}), \quad \forall \mathbf{x} \in S_o$$

which is reduced to

$$0 = -c_j \int_{S_i} H_{ij}(\mathbf{x},\mathbf{y})dS(\mathbf{y}) - d_{jk}\int_{S_i} H_{ij}(\mathbf{x},\mathbf{y})(y_k - \bar{y}_k)dS(\mathbf{y}), \quad \mathbf{x} \in S_o \tag{19}$$

by applying BIE Eq. (10) for $u_i(\mathbf{y})$. The above equation is further reduced to

$$0 = -d_{jk}\int_{S_i} H_{ij}(\mathbf{x},\mathbf{y})(y_k - \bar{y}_k)dS(\mathbf{y}), \quad \mathbf{x} \in S_o$$

for any values of c_i, by applying definition in Eq. (11) and the second identity, Eq. (3) after switching the direction of the normal. Applying the definition in Eq. (11), we can write the above equation as

$$0 = -E_{ilpq}n_l(\mathbf{x})d_{jk}\int_{S_i} \frac{\partial T_{pj}(\mathbf{x},\mathbf{y})}{\partial x_q}(y_k - \bar{y}_k)dS(\mathbf{y}), \mathbf{x} \in S_o$$

or

$$0 = -\frac{1}{2}E_{ilpq}n_l(\mathbf{x})d_{jk}\int_{S_i}\left[\frac{\partial T_{pj}(\mathbf{x},\mathbf{y})}{\partial x_q}(y_k - \bar{y}_k) - \frac{\partial T_{pk}(\mathbf{x},\mathbf{y})}{\partial x_q}(y_j - \bar{y}_j)\right]dS(\mathbf{y}), \quad \mathbf{x} \in S_o$$

by splitting the kernel into two and applying the condition in Eq. (14). This equation is satisfied for any values of d_{jk}, by using the sixth identity, Eq. (8) after reversing the direction of normal n on S_i.

Similarly, substituting $\tilde{u}_i(\mathbf{y})$ into traction BIE Eq. (10) with $\mathbf{x} \in S_i$, we obtain

$$0 = -c_j \int_{S_i} H_{ij}(\mathbf{x},\mathbf{y})dS(\mathbf{y}) - d_{jk}\int_{S_i} H_{ij}(\mathbf{x},\mathbf{y})(y_k - \bar{y}_k)dS(\mathbf{y}), \quad \mathbf{x} \in S_i \tag{20}$$

by applying BIE Eq. (10) for $u_i(\mathbf{y})$. The first integral vanishes for any values of c_i by applying the second identity Eq. (3) and the above equation is reduced to

$$0 = -\frac{1}{2}E_{ilpq}n_l(\mathbf{x})d_{jk}\int_{S_i}\left[\frac{\partial T_{pj}(\mathbf{x},\mathbf{y})}{\partial x_q}(y_k - \bar{y}_k) - \frac{\partial T_{pk}(\mathbf{x},\mathbf{y})}{\partial x_q}(y_j - \bar{y}_j)\right]dS(\mathbf{y}), \quad \mathbf{x} \in S_i \tag{21}$$

as in the previous case. Note that reversing the normal of S_i will not change the sign of the right-hand side of Eq. (21). From the sixth identity Eq. (8), the above expression is further reduced to

$$0 = -\frac{1}{2}E_{ilpq}n_l(\mathbf{x})d_{jk}\frac{1}{2}\left(\delta_{pk}\delta_{jq} - \delta_{pj}\delta_{kq}\right), \quad \mathbf{x} \in S_i$$

or

$$0 = -\frac{1}{2}E_{ijkl}d_{kl}n_j(\mathbf{x}), \quad \mathbf{x} \in S_i \tag{22}$$

which is satisfied for any values of d_{jk} satisfying condition Eq. (14) (In fact, $E_{ijkl}d_{kl}$ is the stress field due to the rigid-body rotation and is indeed zero). Therefore, we must conclude that the solution of traction BIE Eq. (10) can admit arbitrary rigid-body translation and rigid-body rotation terms on the edge of a hole or surface of a void. That is, the solution of the traction BIE Eq. (10) is not unique on the edge of a hole or the surface of a void in multiconnected domain problems.

If one applies a dual BIE formulation using a linear combination of the displacement BIE and traction BIE in the form

$$\text{Displacement BIE} + \beta \times \text{Traction BIE} = 0 \tag{23}$$

where β is a coupling (or weighting) constant, then one arrives at the following equation when collocating on the inner boundary S_i:

$$c_i + d_{ik}(x_k - \bar{y}_k) = -\frac{1}{2}\beta E_{ijkl}d_{kl}n_j(\mathbf{x}), \quad \mathbf{x} \in S_i \tag{24}$$

which is a combination of the result in Eq. (18) for displacement BIE Eq. (9) and the result in Eq. (22) for traction BIE Eq. (10). Again, this equation is satisfied only when $c_i = 0$ and $d_{ik} = 0$. Therefore, the dual BIE does not allow the addition of any rigid-body displacement to the solution on the edge of a hole or the surface of a void. A discussion of the choice of the value for constant β is provided in Sec. 5 where the numerical examples are presented.

The dual BIE is needed in cases when the elastic domain contains both cracks (either open or closed) and holes or voids. The use of either displacement BIE alone or the traction BIE alone will be detrimental as they both have defects, although for different reasons. The displacement BIE degenerates on the crack surfaces, while the traction BIE fails on the edges of holes or surfaces of voids. The dual BIE formulation as proposed in Eq. (23) can remove both defects in the BIEs. The dual BIE formulation as shown in Eq. (24) was originally proposed by Burton and Miller [17] for removing the fictitious eigen frequencies in the BIEs for solving Helmholtz equations in exterior domains, as in acoustic wave problems [18–20]. It has also been found to be very effective and efficient (producing better conditioned BEM systems of equations) for solving various potential, crack and Stokes flow problems [4, 11,12, 21–24].

The defect related to the traction or hypersingular BIEs for multiconnected domains has been reported in Refs. [9,10] for elasticity problems and in Refs. [11,12] for Stokes flow problems, although it has not been proved in a general setting. In Ref. [9], only the constant displacement term is dealt with and an integral representation for the domain enclosed by the hole is applied to determine the unknown constant displacement in the solution on the edge of a hole for the original traction BIE for multidomain problems. A few selected constraints on the edge of the hole are also introduced in order to remove the rigid-body motion in the solution of the traction BIE. In Ref. [10], both the constant and linear terms are discussed, however, only for 2D cases as the integral identities applied are derived only for such cases. It is proposed in Ref. [10] to apply the displacement BIE in the Galerkin BEM, instead of the traction BIE, on the traction-free edge of a hole, in order to avoid the nonuniqueness of the displacement solution of the traction BIE. For Stokes flow problems, a dual BIE formulation using a linear combination of the singular and hypersingular BIEs is suggested in Refs. [11,12]. However, the theoretical proof of the nonunique solution and reasoning of the remedy are not provided in Refs. [11,12].

4 Matrix Interpretation of the Nonuniqueness of the Solution of the Discretized Traction BIE for Multiconnected Domains

In this section, we further demonstrate the nonuniqueness of the traction BIE using the discretized or matrix equations. The nonuniqueness of the solution of a discretized integral equation is

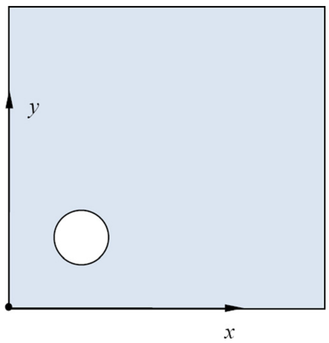

Fig. 3 A square plate with one circular hole

indicated by the nonempty null space of the relevant influence matrices. Denote the discretized systems of integral equations, Eqs. (9) and (10), by

$$[\mathbf{G}]\{\mathbf{t}\} = [\mathbf{T}]\{\mathbf{u}\} \tag{25}$$

and

$$[\mathbf{L}]\{\mathbf{t}\} = [\mathbf{M}]\{\mathbf{u}\} \tag{26}$$

respectively. Consider first the case in which the domain contains only one hole or void. By grouping the nodal displacements and tractions of the outer and inner boundaries separately, system Eq. (25) can be re-arranged as

$$\begin{bmatrix} \mathbf{G}_{oo} & \mathbf{G}_{oi} \\ \mathbf{G}_{io} & \mathbf{G}_{ii} \end{bmatrix} \begin{Bmatrix} \mathbf{t}_o \\ \mathbf{t}i \end{Bmatrix} \begin{bmatrix} \mathbf{T}_{oo} & \mathbf{T}_{oi} \\ \mathbf{T}_{io} & \mathbf{T}_{ii} \end{bmatrix} \begin{Bmatrix} \mathbf{u}_o \\ \mathbf{u}i \end{Bmatrix} \tag{27}$$

where the subscripts "o" and "i" refer to the outer and the inner boundaries respectively. It is well known that for a Neumann problem, the solution of Eq. (25) is not uniquely defined. Hence matrix $[\mathbf{T}]$ is singular. For 2D problems, $[\mathbf{T}]$ should contain three null vectors, corresponding to the three rigid-body modes of the multiconnected domain. Similarly $[\mathbf{T}_{oo}]$ is also singular with its three null vectors being the three rigid-body modes of the solid domain enclosed by the outer boundary. $[\mathbf{T}_{ii}]$, on the other hand, is nonsingular. One can regard it as the influence matrix resulting from the discretized displacement BIE of an exterior domain outside the hole or void, which does not admit any rigid-body motion. In Sec. 3, it is proved that the displacement BIE Eq. (9) does not have a solution of which the inner hole undergoes a rigid-body motion while the outer boundary remains stationary, i.e.,

$$\{\mathbf{u}\} = \begin{Bmatrix} o \\ \tilde{\mathbf{u}}_i \end{Bmatrix}$$

where $\tilde{\mathbf{u}}_i$ represents the rigid-body mode of the inner hole. Such a fact can also be explained by the fact that $[\mathbf{T}_{ii}]$ is nonsingular; hence when it is multiplied with a rigid-body displacement vector, a nonzero vector results, which is not admissible.

For Eq. (26), the situation is different. In addition to the three physical rigid-body modes, $[\mathbf{M}]$ has additional three null vectors corresponding to $\{\mathbf{u}\} = \begin{Bmatrix} o \\ \tilde{\mathbf{u}}_i \end{Bmatrix}$. Again, Eq. (26) can be re-arranged as

$$\begin{bmatrix} \mathbf{L}_{oo} & \mathbf{L}_{oi} \\ \mathbf{L}_{io} & \mathbf{L}_{ii} \end{bmatrix} \begin{Bmatrix} \mathbf{t}_o \\ \mathbf{t}i \end{Bmatrix} = \begin{bmatrix} \mathbf{M}_{oo} & \mathbf{M}_{oi} \\ \mathbf{M}_{io} & \mathbf{M}_{ii} \end{bmatrix} \begin{Bmatrix} \mathbf{u}_o \\ \mathbf{u}i \end{Bmatrix} \tag{28}$$

Unlike $[\mathbf{T}_{ii}]$, the matrix $[\mathbf{M}_{ii}]$ is singular and has three null vectors described by $\tilde{\mathbf{u}}i$ based on the proof of Eq. (20). The singularity stems from the nature of the kernel itself, and does not seem to correspond to any physical mode of the problem. Moreover, the

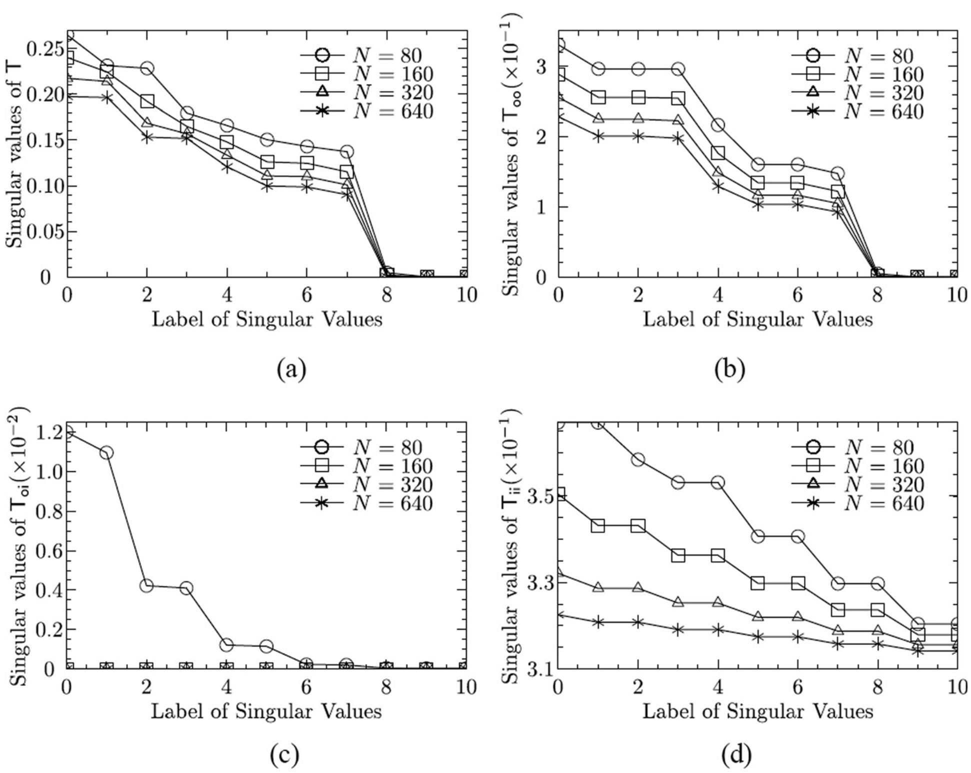

Fig. 4 The last several singular values of the influence matrix $[\mathbf{T}]$ and its submatrices. The singular values are labeled consecutively using integer numbers. Circles, squares, triangles and stars represent the values obtained from meshes with 80, 160, 320, and 640 elements respectively. With the mesh of 640 elements, the condition numbers of $[\mathbf{T}]$, $[\mathbf{T}_{oo}]$,$[\mathbf{T}_{oi}]$ and $[\mathbf{T}_{ii}]$ shown in (*a*), (*b*), (*c*) and (*d*), respectively are 2.9×10^6, 1.8×10^6, 3.0×10^7 and 3.2.

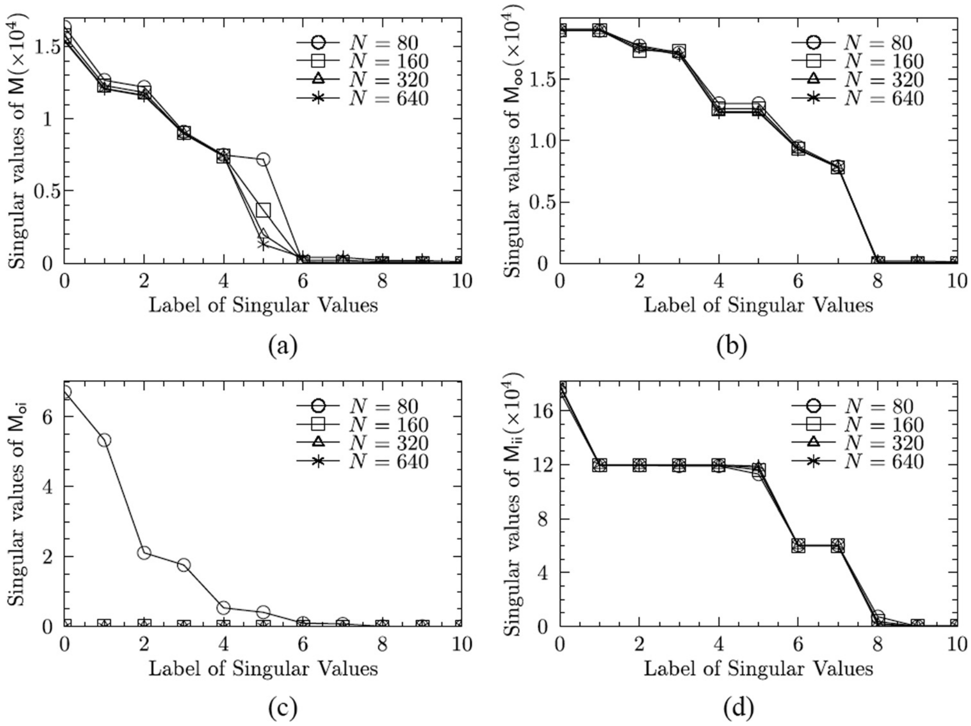

Fig. 5 The last several singular values of the influence matrix [M] and its submatrices. The singular values are labeled consecutively using integer numbers. Circles, squares, triangles and stars represent the values obtained from meshes with 80, 160, 320, and 640 elements respectively. With the mesh of 640 elements, the condition numbers of [M], [M_{oo}],[M_{oi}] and [M_{ii}] shown in (*a*), (*b*), (*c*) and (*d*), respectively are 3.0×10^4, 1.5×10^4, 5.8×10^7 and 7.4×10^3.

null space of the submatrix $[\mathbf{M}_{oi}]$ is also nonempty, containing the three null vectors $\tilde{\mathbf{u}}i$ based on the proof of Eq. (19). With both $[\mathbf{M}_{ii}]$ and $[\mathbf{M}_{oi}]$ being singular, it is not difficult to conclude that $[\mathbf{M}]$ is also singular and contains six null vectors.

For a general case in which the problem domain contains N inner holes or voids, Eq. (26) can be expanded as

$$\begin{bmatrix} \mathbf{L}_{oo} & \mathbf{L}_{oi_1} & \dots & \mathbf{L}_{oi_N} \\ \mathbf{L}_{i_1o} & \mathbf{L}_{i_1i_1} & \dots & \mathbf{L}_{i_1i_N} \\ \vdots & \vdots & & \vdots \\ \mathbf{L}_{i_No} & \mathbf{L}_{i_Ni_1} & \dots & \mathbf{L}_{i_Ni_N} \end{bmatrix} \begin{Bmatrix} \mathbf{t}_o \\ \mathbf{t}_{i_1} \\ \vdots \\ \mathbf{t}_{i_N} \end{Bmatrix} = \begin{bmatrix} \mathbf{M}_{oo} & \mathbf{M}_{oi_1} & \dots & \mathbf{M}_{oi_N} \\ \mathbf{M}_{i_1o} & \mathbf{M}_{i_1i_1} & \dots & \mathbf{M}_{oi_N} \\ \vdots & \vdots & & \vdots \\ \mathbf{M}_{i_No} & \mathbf{M}_{i_Ni_1} & \dots & \mathbf{M}_{i_Ni_N} \end{bmatrix} \begin{Bmatrix} \mathbf{u}_o \\ \mathbf{u}_{i_1} \\ \vdots \\ \mathbf{u}_{i_N} \end{Bmatrix} \quad (29)$$

where the subscript "$i_k, k = 1, 2, \cdots N$" denotes the kth inner hole. Based on the identities presented in Sec. 2, it can be easily shown that

$$[\mathbf{M}_{oi_k}]\{\tilde{\mathbf{u}}_{i_k}\} = 0 \quad (30)$$

and

$$[\mathbf{M}_{i_ji_k}]\{\tilde{\mathbf{u}}_{i_k}\} = 0 \quad (31)$$

where $\{\tilde{\mathbf{u}}_{i_k}\}$ is the displacement vector corresponding to the rigid-body mode of the kth inner hole and $j, k = 1, 2, \cdots N$. Hence, $[\mathbf{M}]$ has $3N + 3$ independent null vectors, of which three are the rigid-body modes of the multiconnected domain. The remaining $3N$ vectors, resulting from the properties of the kernel, can be expressed as $\{ 0 \quad 0 \quad \cdots \quad \tilde{\mathbf{u}}_{i_k} \quad \cdots \quad 0 \}, k = 1, 2 \cdots N$.

5 Numerical Examples

In this section, several 2D examples are presented to demonstrate the uniqueness properties of the displacement, traction and dual BIE solutions. In all the cases, Young's modulus is 227KPa and Poisson's ratio is 0.2. All boundary integral equations are solved numerically using the collocation method with constant elements. Evaluation of the influence matrices is performed analytically following the formulas provided in Ref. [12]. As mentioned in Sec. 4, the nonuniqueness of the solution of a discretized integral equation is reflected in the null space of the relevant influence matrices, which is equivalent to the existence of zero singular values of the corresponding influence matrices. Therefore, the null spaces of these matrices are examined via singular value decomposition.

5.1 Example 1: A Square Plate With One Circular Hole. As the first example, a square plate with a circular hole as sketched in Fig. 3 is considered. The edge length of the square plate is set to be 10 and the radius of the hole is 1. The influence matrices $[\mathbf{T}]$ and $[\mathbf{M}]$ defined in Eqs. (25) and (26) are evaluated and the singular values of these matrices and their submatrices are examined. Four different mesh sizes corresponding to a total of 80, 160, 320, and 640 elements are employed. Figure 4 plots the last several singular values of matrix $[\mathbf{T}]$ and its submatrices $[\mathbf{T}_{oo}]$, $[\mathbf{T}_{oi}]$ and $[\mathbf{T}_{ii}]$. It is evident from these plots that both $[\mathbf{T}]$ and $[\mathbf{T}_{oo}]$ have three near zero singular values, while $[\mathbf{T}_{ii}]$ has none, which are consistent with the analysis provided in Sec. 4. The near zero singular values decrease with the increased element numbers and approach to zero when the mesh size approaches to zero. It is interesting to note that the submatrix $[\mathbf{T}_{oi}]$ has many near zero singular values in addition to the three corresponding to the rigid-body modes of the inner hole. In fact, the condition number of $[\mathbf{T}_{oi}]$ is close to 3×10^7, one order higher than that of $[\mathbf{T}]$ and $[\mathbf{T}_{oo}]$. Similar behavior has also been observed for $[\mathbf{T}_{io}]$. These observations can be explained by considering first identity in Eq. (2) for the traction T kernel.

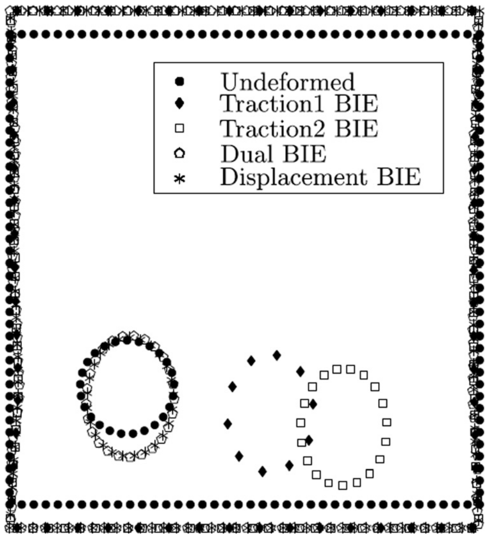

Fig. 6 The shapes of the plate before and after deformation. The circles show the plate before deformation, and the stars and pentagons represent the deformed shapes obtained from the displacement BIE and dual BIE, respectively. The points marked as diamonds and squares illustrate the two deformed shapes obtained with two different meshes from the traction BIE.

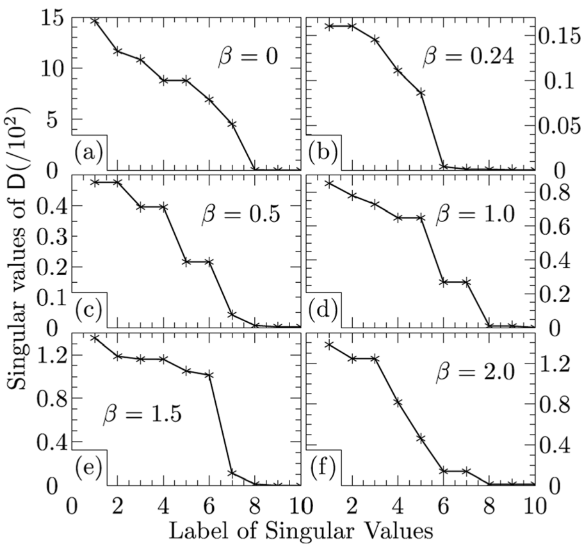

Fig. 7 The effect of β on the performance of the dual BIE formulation: the last ten singular values of [D] at a few selected β values

The last several singular values of matrices $[\mathbf{M}]$ and its submatrices $[\mathbf{M}_{oo}]$, $[\mathbf{M}_{oi}]$ and $[\mathbf{M}_{ii}]$ are plotted in Fig. 5. Similar to the behavior of $[\mathbf{T}_{oo}]$, $[\mathbf{M}_{oo}]$ has three null vectors corresponding to the rigid-body modes of the square plate. But unlike $[\mathbf{T}_{ii}]$ which is nonsingular, $[\mathbf{M}_{ii}]$ has three zero singular values. As a consequence, $[\mathbf{M}]$ has six singular values as clearly indicated in Fig. 5(*a*). All these results agree very well with the theoretical predictions presented in Secs. 3 and 4. The behavior of $[\mathbf{M}_{oi}]$ is similar to that of $[\mathbf{T}_{oi}]$. The condition number of $[\mathbf{M}_{oi}]$ is also on the order of 10^7, much higher than that of $[\mathbf{M}]$ and $[\mathbf{M}_{ii}]$. This can be explained by considering second identity in Eq. (3) for the H kernel.

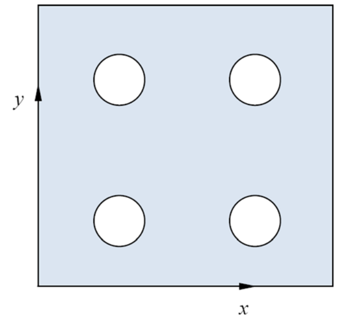

Fig. 8 A schematic of a plate with four circular holes

To further demonstrate the nonuniqueness of the traction BIE solution, the deformation of a plate with a hole under a uniform stretch of 0.01 applied on both the top and the bottom edges of the plate as illustrated in Fig. 6 is calculated from both the displacement BIE and traction BIE. The undeformed shape is indicated by the solid circles and the stars represent the deformed shape obtained from the displacement BIE. Both diamonds and squares mark the two solutions obtained from the traction BIE with two different mesh sizes, illustrating the nonuniqueness of the traction BIE solution.

As suggested in Sec. 3, a remedy to the nonuniqueness problem of the traction BIE is to employ a dual BIE formulation. We set the weighting factors of the normalized displacement BIE and traction BIE be 1 and β, respectively. The null space of the influence matrix, $[\mathbf{D}] = [\mathbf{T}] + \beta(h/E)[\mathbf{M}]$, where h is the nominal mesh size, of the dual BIE is examined for various values of β in the range of $0 \le \beta \le 2$. Figure 7 plots ten smallest singular values of $[\mathbf{D}]$ for a few selected weighting factors. Although theoretically matrix $[\mathbf{D}]$ only has three zero singular values for any β, due to numerical errors, the performance of the hybrid scheme varies with the choice of β. In some cases; for example, the case indicated in Fig. 7(*b*), the fourth smallest singular value is very close to zero. Hence, the performance of the dual BIE formulation may not be as good as expected in those cases. To examine the accuracy of the dual BIE formulation and the influence of the β value, the plate problem with one hole is solved again using the dual BIE formation with several different β values. The deformed shape of the plate obtained from the dual BIE with $\beta = 1$ is shown in Fig. 6 indicated by pentagons, which matches with the shape obtained from the displacement BIE quite well. Table 1 lists the L^2-norm errors of the calculated displacements obtained from both the displacement BIE and the dual BIE formulations at different mesh sizes. Due to the lack of the analytic solution of the problem, the benchmark solution is obtained using the displacement BIE approach with a finer mesh of 2240 constant elements. Overall, the accuracy of the dual BIE formulation is worse than that of the displacement BIE formulation, and the weighting factor does has

Table 1 L^2-norm errors in the simulated boundary displacements of the plate with one hole obtained from both the dual BIE and the displacement BIE formulations

Number of elements	Displacement BIE	Dual BIE ($\beta = 0.24$)	Dual BIE ($\beta = 1.0$)	Dual BIE ($\beta = 2.0$)
140	0.0210941	0.0364847	0.0881613	0.0325696
280	0.0083812	0.0442276	0.0522068	0.0180375
560	0.0031254	0.0125011	0.0177214	0.0118584
1120	0.0009345	0.0094700	0.0066303	0.0192113

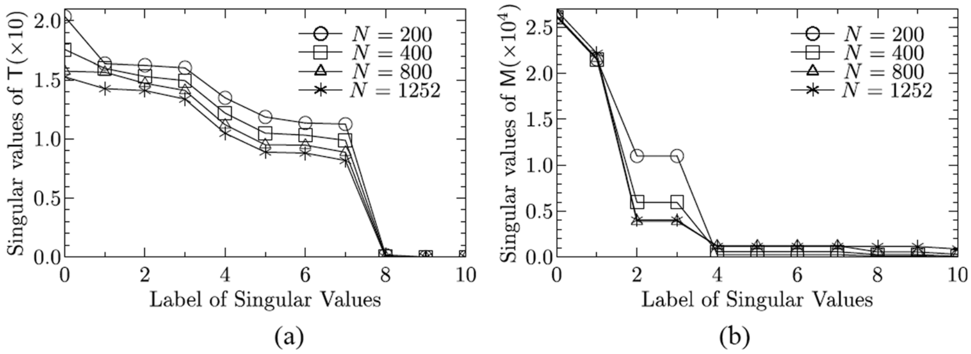

Fig. 9 The last several singular values of matrices [T] shown in (*a*) and [M] shown in (*b*) for the plate with two holes. The circles, squares, triangles and stars represent the values obtained from meshes with 200, 400, 800 and 1252 elements, respectively.

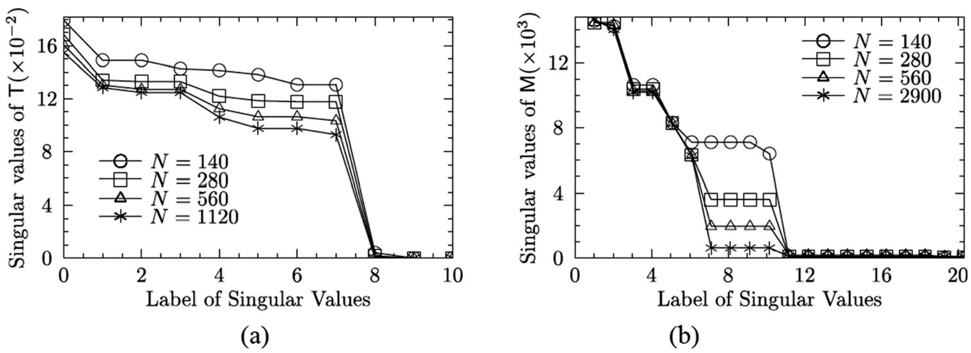

Fig. 10 The last several singular values of matrices [T] shown in (*a*) and [M] shown in (*b*) for the plate with four holes. The circles, squares, triangles and stars represent the values obtained from meshes with 140, 280, 560 and 2900 elements, respectively.

an influence on the accuracy of the results. The case with $\beta = 1$ performs the best, which is consistent with the singular values plotted in Fig. 7.

5.2 Example 2: A Square Plate With Several Circular Holes. To illustrate the correlation between the number of the inner holes and the number of the null vectors of matrix $[\mathbf{M}]$, square plates with two and four inner holes are considered. A schematic of the plate with four circular holes is illustrated in Fig. 8. Figures 9 and 10 present the last several singular values of matrices $[\mathbf{T}]$ and $[\mathbf{M}]$ obtained at different discretized levels for the two cases. While the number of zero singular values of matrix $[\mathbf{T}]$ is always three regardless of the number of the inner holes, the number of the null vectors of $[\mathbf{M}]$ increases with the number of the holes and clearly follows $3N + 3$ pattern, where N is the number of the inner holes, which is consistent with the analysis given in Sec. 4.

6 Conclusion

The six integral identities, including the two derived in this paper, satisfied by the fundamental solution for elastostatic problems, are employed to theoretically investigate the uniqueness of the displacement and traction BIE solutions for multiconnected domains in a general setting. It is shown both in the continuous and discretized spaces that the displacement (singular) BIE does not allow any rigid-body displacement terms, while the traction BIE can have arbitrary rigid-body translation and rotation terms, in the BIE solutions on the edge of a hole or the surface of a void. Hence the displacement solution from the traction BIE is not unique. The dual BIE formulation can theoretically remedy the nonuniqueness problem of the traction BIE. The weighting factor of the normalized traction BIE, however, has to be chosen carefully and need further investigation. It is demonstrated that a unit weighting factor works very well for the examples studied.

Acknowledgment

The paper was prepared while the first author was on sabbatical leave from the University of Cincinnati and visiting the Department of Mechanical Engineering of Hong Kong University of Science and Technology (HKUST). He would like to thank Professor Wenjing Ye at HKUST for hosting the visit. The second and third authors would like to acknowledge Hong Kong Research Grants Council for supporting a part of this work under Competitive Earmarked Research Grant 621411.

References

[1] Rizzo, F. J., 1967, "An Integral Equation Approach to Boundary Value Problems of Classical Elastostatics," Q. Appl. Math., **25**, pp. 83–95.
[2] Liu, Y. J., Mukherjee, S., Nishimura, N., Schanz, M., Ye, W., Sutradhar, A., Pan, E., Dumont, N.A., Frangi, A., and Saez, A., 2011, "Recent Advances and Emerging Applications of the Boundary Element Method," ASME Appl. Mech. Rev., **64**, pp. 1–38.
[3] Chen, J. T., Kou, S. R., and Lin, J. H., 2002, "Analytic Study and Numerical Experiments for Degenerate Scale Problems in the Boundary Element Method for Two-Dimensional Elasticity," Int. J. Numer. Methods Eng., **54**, pp. 1669–1681.
[4] Krishnasamy, G., Rizzo, F. J., and Liu, Y. J., 1994, "Boundary Integral Equations for Thin Bodies," Int. J. Numer. Methods Eng., **37**, pp. 107–121.
[5] Liu, Y. J., 1998, "Analysis of Shell-Like Structures by the Boundary Element Method Based on 3-D Elasticity: Formulation and Verification," Int. J. Numer. Methods Eng., **41**, pp. 541–558.
[6] Liu Y. J., and Rudolphi, T. J., 1991, "Some Identities for Fundamental Solutions and Their Applications to Weakly-Singular Boundary Element Formulations," Eng. Anal. Boundary Elements, **8**, pp. 301–311.
[7] Liu Y. J., and Rudolphi, T. J., 1999, "New Identities for Fundamental Solutions and Their Applications to Non-Singular Boundary Element Formulations," Comput. Mech., **24**, pp. 286–292.

[8] Liu, Y. J., 2000, "On the Simple-Solution Method and Non-Singular Nature of the BIE/BEM—A Review and Some New Results," Eng. Anal. Boundary Elements, **24**(10), pp. 789–795.
[9] Frangi, A., and Novati, G., 1996, "Symmetric BE Method in Two-Dimensional Elasticity: Evaluation of Double Integrals for Curved Elements," Comput. Mech., **19**, pp. 58–68.
[10] Perez-Gavilan, J. J., and Aliabadi, M. H., 2001, "Symmetric Galerkin BEM for Multi-Connected Bodies," Commun. Numer. Methods Eng., **17**, pp. 761–770.
[11] Liu, Y. J., 2008, "A New Fast Multipole Boundary Element Method for Solving 2-D Stokes Flow Problems Based on a Dual BIE Formulation," Eng. Anal. Boundary Elements, **32**, pp. 139–151.
[12] Liu, Y. J., 2009, *Fast Multipole Boundary Element Method—Theory and Applications in Engineering*, Cambridge University, Cambridge.
[13] Cruse, T. A., 1974, "An Improved Boundary-Integral Equation Method for Three Dimensional Elastic Stress Analysis," Comput. Struct., **4**, pp. 741–754.
[14] Rizzo, F. J., and Shippy, D. J., 1977, "An Advanced Boundary Integral Equation Method for Three-Dimensional Thermoelasticity," Int. J. Numer. Methods in Eng., **11**, pp. 1753–1768.
[15] Rudolphi, T. J., 1991, "The Use of Simple Solutions in the Regularization of Hypersingular Boundary Integral Equations," Math. Comput. Modell., **15**, pp. 269–278.
[16] Liu, Y. J., and Rizzo, F. J., 1993, "Hypersingular Boundary Integral Equations for Radiation and Scattering of Elastic Waves in Three Dimensions," Comput. Methods Appl. Mech. Eng., **107**, pp. 131–144.
[17] Burton, A. J., and Miller, G. F., 1971, "The Application of Integral Equation Methods to the Numerical Solution of Some Exterior Boundary-Value Problems," Proc. R. Soc. London, Ser. A, **323**, pp. 201–210.
[18] Liu, Y. J., and Rizzo, F. J., "A Weakly-Singular Form of the Hypersingular Boundary Integral Equation Applied to 3-D Acoustic Wave Problems," Comput. Methods Appl. Mech. Eng., **96**, pp. 271–287.
[19] Liu, Y. J., and Chen, S. H., 1999, "A New Form of the Hypersingular Boundary Integral Equation for 3-D Acoustics and its Implementation With C^0 Boundary Elements," Comput. Methods Appl. Mech. Eng., **173**, pp. 375–386.
[20] Liu, Y. J., and Shen, L., 2007, "A Dual BIE Approach for Large-Scale Modeling of 3-D Electrostatic Problems With the Fast Multipole Boundary Element Method," Int. J. Numer. Methods Eng., **71**, pp. 837–855.
[21] Liu, Y. J., and Rizzo, F. J., 1997, "Scattering of Elastic Waves From Thin Shapes in Three Dimensions Using the Composite Boundary Integral Equation Formulation," J. Acoust. Soc. Am., **102**(2), pp. 926–932.
[22] Aliabadi, M. H., 2002, *The Boundary Element Method—Vol. 2 Applications in Solids and Structures*, Wiley, Chichester, UK.
[23] Liu, Y. J., 2006, "Dual BIE Approaches for Modeling Electrostatic MEMS Problems With Thin Beams and Accelerated by the Fast Multipole Method," Eng. Anal. Boundary Elements, **30**, pp. 940–948.
[24] Frangi, A., 2005, "A Fast Multipole Implementation of the Qualocation Mixed-Velocity-Traction Approach for Exterior Stokes Flows," Eng. Anal. Boundary Elements, **29**, pp. 1039–1046.